Hindawi Publishing Corporation
Journal of Nanomaterials
Volume 2015, Article ID 527070, 6 pages
http://dx.doi.org/10.1155/2015/527070

Research Article

Visible-Light Photocatalytic Activity of N-Doped TiO_2 Nanotube Arrays on Acephate Degradation

Xinlei Zhang,[1,2] Juan Zhou,[3] Yufen Gu,[1] and Ding Fan[1]

[1]*State Key Laboratory of Gansu Advanced Nonferrous Metal Materials, Lanzhou University of Technology, Lanzhou 730050, China*
[2]*Key Laboratory of Rare Earth Functional Materials and Applications, Zhoukou Normal University, Zhoukou 466001, China*
[3]*College of Chemistry and Chemical Engineering, Zhoukou Normal University, Zhoukou 466001, China*

Correspondence should be addressed to Xinlei Zhang; xinleizh@126.com

Received 24 July 2014; Accepted 15 August 2014

Academic Editor: Shifeng Zhou

Highly ordered nitrogen-doped titanium dioxide (N-doped TiO_2) nanotube arrays were prepared by anodic oxidation method and then annealed in a N_2 atmosphere to obtain N-doped TiO_2 nanotube arrays. The samples were characterized with scanning electron microscope (SEM), X-ray powder diffraction (XRD), X-ray photoelectron spectrum (XPS), and UV-visible spectrophotometry (UV-vis) spectrum. Degradation of the insecticide acephate under the visible light was used as a model to examine the visible-light photocatalytic activity of N-doped TiO_2 nanotube arrays. The results show that N type doping has no notable effects on the morphology and structure of TiO_2 nanotube arrays. After N type doping, the N replaces a small amount of O in TiO_2, forming an N–Ti–O structure. This shifts the optical absorption edge and enhances absorption of the visible light. N-doped TiO_2 nanotube arrays subjected to annealing at 500°C in N_2 atmosphere show the strongest photocatalytic activity and reach a degradation rate of 84% within 2 h.

1. Introduction

Highly ordered TiO_2 nanotube arrays prepared by electrochemical anodic oxidation not only have the advantages of traditional TiO_2 including high catalytic activity, nontoxicity, and long-term photostability [1], but also offer a large surface area, excellent dielectric properties, and strong adsorption capacity. Thus, TiO_2 nanotube arrays is the green photocatalyst with the most promising development prospects [2]. However, TiO_2 nanotube arrays are subject to their own limitations, just like traditional TiO_2. TiO_2 is a large bandgap semiconductor that is commonly investigated in rutile (bandgap 3.0 eV) and anatase (bandgap 3.2 eV) phase. It needs UV light excitation to produce photocatalytic activity. Visible light of lower energy than UV light cannot be absorbed by TiO_2 nanotube arrays, and thus the utilization of the sunlight is low, limiting their practical application. Therefore, an important goal is to broaden the range of the visible light to which TiO_2 nanotube arrays respond and enhance their photocatalytic activity under the visible light.

Previous studies have found that the appropriate doping or surface modification of TiO_2 nanotube arrays, such as nonmetallic element doping [3], metal ion doping [4], surface deposition of precious metals [5, 6], semiconductor modifications [7, 8], and dye-sensitization [9], can effectively broaden the response range of TiO_2 nanotube arrays to the visible light and thus increase their visible-light photocatalytic activity. Nonmetallic element doping has attracted a particularly high research interest. Indeed, replacing a small amount of lattice oxygen in TiO_2 with nonmetallic elements (B, N, F, and C) can narrow the bandgap of TiO_2 and expand the photocatalytic spectral response range to the visible light without reducing the response to the UV light [10]. There are currently many methods for doping N in TiO_2 nanotube arrays including heat treatment in NH_3 flow [3], chemical vapor deposition [11], and wet impregnation [12, 13]. With all of these methods, nonmetal elemental N can be successfully doped into the TiO_2 lattice enhancing its response to the visible spectrum. Vitiello et al. [14] put TiO_2 nanotube arrays in NH_3 flow and obtained N-doped TiO_2 nanotube arrays;

the morphology of the nanotubes was not destroyed and XPS characterization indicated that N was successfully doped into the TiO_2 lattice. The ultraviolet and visible-light photocurrent densities of the product were significantly improved versus undoped sample. Shankar et al. [15] realized N doping during TiO_2 nanotube array preparation and expanded the response spectrum to 400–530 nm.

In the present study, N-doped TiO_2 nanotube arrays were prepared using anodic oxidation and calcination in N_2 atmosphere. Their structure was analyzed with a variety of analytical tools. Acephate, which is difficult to be degraded, was used as a model to examine the photocatalytic activity of the prepared N-doped TiO_2 nanotube arrays under the visible light.

2. Experimental

2.1. Preparation of N-Doped TiO_2 Nanotube Arrays. Anodization experiments were performed in a two-electrode configuration with treated titanium as the anode and platinum as the counter electrode, respectively [2]. Both electrodes were immersed in 100 mL inorganic electrolyte containing 0.5 wt.% NaF and 0.1 mol/L H_2SO_4. The direct voltage was 20 V. At this constant voltage the oxidation reaction proceeded for 1 h. The sample was then rinsed with distilled water to obtain highly ordered nanotube arrays. The prepared TiO_2 nanotube film was placed in a tube furnace. It was annealed in N_2 atmosphere for 2 h at different temperatures to obtain N-doped TiO_2 nanotube arrays.

2.2. Characterization of N-Doped TiO_2 Nanotube Arrays. A Quanta200 scanning electron microscope (FEI Company, Netherlands) was used for morphological analysis of the samples. A D8 Focus X-ray powder diffraction system (BRUKER Company, Germany) was used to examine the crystal structure of the samples. The energy dispersion was measured with a Sol-X detector. An ESCALAB MK type II X-ray photoelectron spectroscope (VG Instrument, UK) was used to test surface elements and the chemical status of the elements. A Lambda35 UV-visible spectrophotometer with an integrating sphere (PerkinElmer, USA) was used to measure the UV-visible diffuse reflectance spectra of the samples.

2.3. Visible-Light Photocatalytic Activity on Acephate Degradation. Sunlight was used as the visible light, and nanotube arrays film was placed in a beaker containing 20 mL 8×10^{-4} mol/L solution of organophosphorus pesticide acephate. The beaker was placed in a darkroom and subjected to magnetic stirring for 30 min to achieve adsorption equilibrium. A certain amount of H_2O_2 was added, and the beaker was then placed under the sunlight with sampling at 30 min intervals. The UV-visible spectrophotometer (PerkinElmer, USA) was used to measure the absorbance of the solution at 270 nm, and the degradation rate was calculated according to the following formula:

$$\eta = \frac{A_0 - A_t}{A_0} \times 100\%, \quad (1)$$

where η stands for the photodegradation rate of acephate, while A_0 is the initial absorbance of the suspension which attained an adsorption-desorption equilibrium before photodegradation and A_t is the final absorbance.

3. Results and Discussion

3.1. SEM Analysis. Figure 1 shows front view SEM images of TiO_2 nanotube arrays (Figure 1(a)) and N-doped TiO_2 nanotube arrays (Figures 1(b)–1(d)) annealed at different temperatures in air and N_2. After being annealed at 400°C, the surfaces of both the undoped and N-doped nanotubes exhibited a perpendicular, orderly tubular structure. The tube bore was clean and smooth, with a diameter of about 40 nm and a wall thickness of 12 nm. This suggests that N doping does not markedly impact the morphology of the TiO_2 nanotubes. As the annealing temperature increased, the nanotube diameter decreased, the tube wall thickness increased, and the tube opening became coarser.

Figure 2 shows the cross-sectional SEM images of TiO_2 nanotube arrays (Figure 2(a)) and N-doped TiO_2 nanotube arrays (Figure 2(b)) annealed at 400°C. The TiO_2 nanotube wall was smooth, and there was no intertwining between the tubes; the opening nanotubes were at the front and the bottom was a closed hemispherical dome structure. The N-doped TiO_2 nanotube wall was coarse and the tubes aggregated. Some tubular structure showed wall rupture.

3.2. XRD Analysis. Figure 3 illustrates the XRD patterns of TiO_2 nanotube arrays and N-doped TiO_2 nanotube arrays after being annealed at different temperatures. The nonannealed sample only showed Ti characteristic diffraction peaks (JCPDS 44-1294) at 38.46°, 40.22°, 53.04°, and 71.02° (Figure 3(a)), suggesting that TiO_2 nanotube arrays prepared by anodic oxidation were amorphous. After being annealed in the air or N_2 atmosphere, the anatase phase TiO_2 characteristic peaks (JCPDS 21-1272) were found at 25.47°, 37.80°, 48.05°, and 63.40°, suggesting that TiO_2 had changed from the amorphous phase into the anatase phase. Figure 3(b) shows the comparison of crystal face diffraction peaks between the anatase phase TiO_2 and N-doped TiO_2 (101) nanotube arrays. The N doping made the crystal face diffraction peaks of the anatase phase TiO_2 (101) substantially shift to 2θ, and the peaks became broader with reduced peak area. This may be because compressive strain increases as N replaces O in the TiO_2 structure due to differences in binding properties [16]. After being annealed at 600°C in a N_2 atmosphere, rutile peaks (JCPDS 21-1276) appeared at 27.3°, 36.15°, 41.02°, and 54.43° characteristic of TiO_2, as shown in Figure 3(f). No other phases were found in the diffraction peaks, suggesting that N doping does not form new substances.

3.3. XPS Analysis. Figure 4(a) shows the XPS of N-doped TiO_2 nanotube arrays. The characteristic peaks were C1s at 284.8 eV, N1s at 398.2 eV, Ti2p at 458.6 eV, O1s at 532.8 eV, and Ti2s at 561.2 eV. The C1s peak corresponds to the C–H bond and C–C bond in the hydrocarbon, which was from carbon

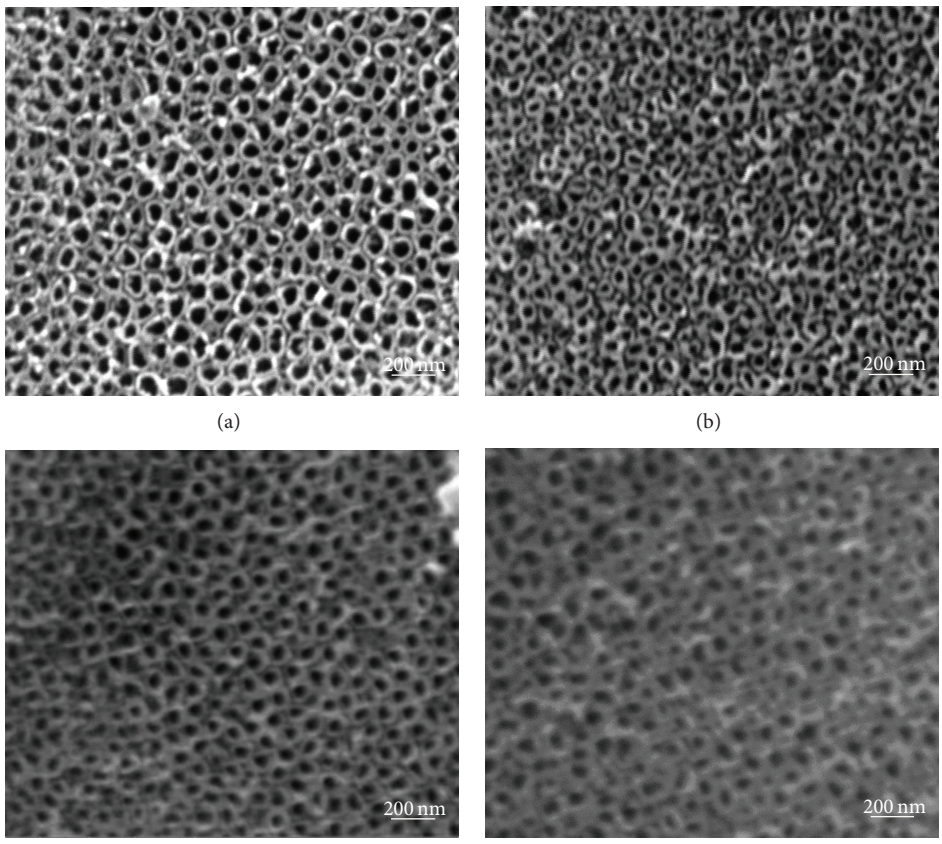

(a) (b)

(c) (d)

Figure 1: SEM top-view images of (a) TiO_2 nanotube arrays annealed at 400°C and N-doped TiO_2 nanotube arrays annealed at various temperatures, (b) 400°C, (c) 500°C, and (d) 600°C.

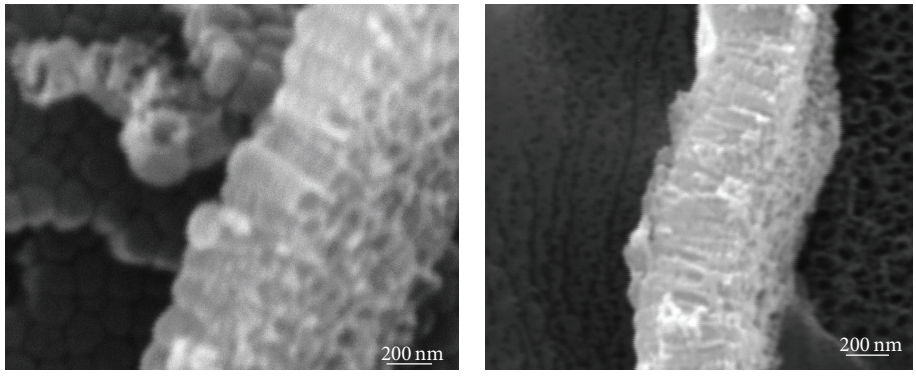

(a) (b)

Figure 2: SEM cross-section view images of the (a) TiO_2 and (b) N-doped TiO_2 nanotube arrays annealed at 400°C.

contamination as the sample was exposed to air or X-ray photoelectron spectroscope during testing. There is a broad N1s characteristic peak in the XPS spectrum of N1s at 398.2 eV (Figure 4(b)). The N was doped into the TiO_2 system, with a valence of −3, and replaced part of the O atoms to form an N–Ti–O bond. Ohno et al. [17] reported that the N1s binding energy in Ti–N was 397.2 eV. The electron binding energy was higher here because the electron binding energy of N in the N–Ti–O structure is higher than that of N in the N–Ti–N structure. This is due to the higher electronegativity of O than N, and the electron density of N in the N–Ti–O structure is higher than that of N in the N–Ti–N structure. Figure 4(c) shows local amplification of the XPS spectrum at Ti2p. The Ti2p peaks were symmetrically distributed around 458.6 eV and 464.4 eV, corresponding to Ti^{4+} in TiO_2. The Ti element had a valence of +4. This indicates that, in N-doped TiO_2,

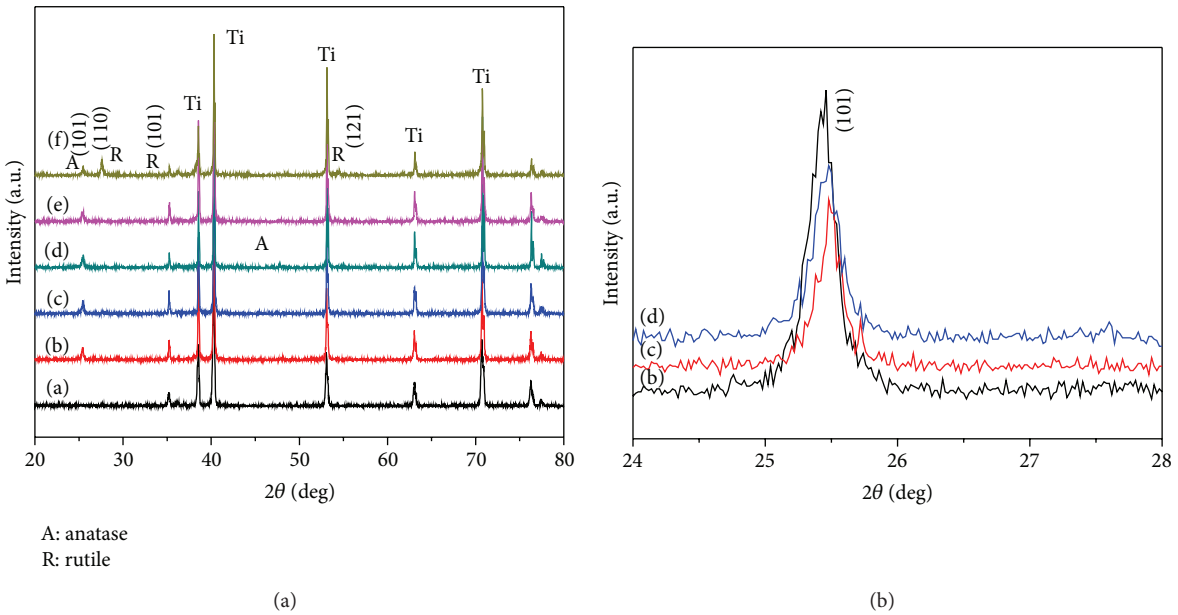

FIGURE 3: XRD patterns of the pure TiO_2 nanotube arrays and N-doped TiO_2 nanotube arrays annealed at temperatures ranging from 300 to 600°C. Pure TiO_2 nanotube array films: (a) before annealing, (b) at 300°C. N-doped TiO_2 nanotube array films: (c) 300°C, (d) 400°C, (e) 500°C, and (f) 600°C.

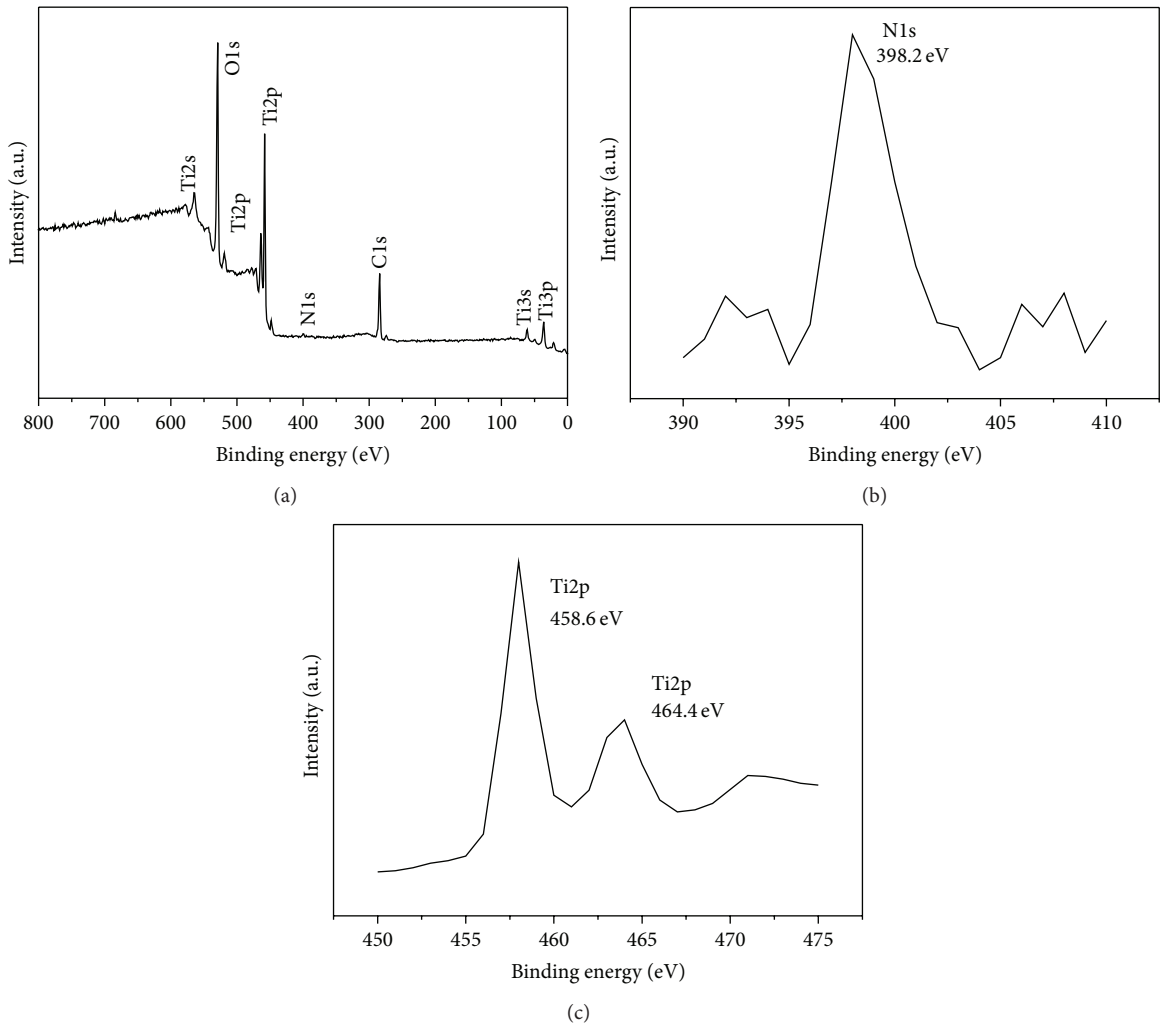

FIGURE 4: XPS patterns of N-doped TiO_2 nanotube arrays, (a) XPS survey spectrum, (b) N1s and (c) Ti2p.

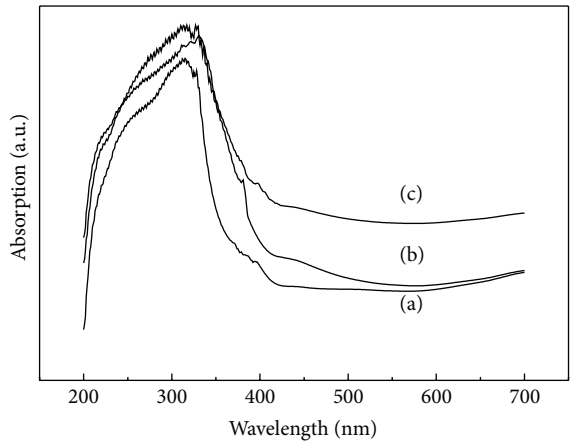

FIGURE 5: UV-vis absorption spectra of different samples, (a) pure TiO_2 nanotube arrays annealed at 400°C and N-TiO_2 nanotube arrays annealed at (b) 400°C and (c) 500°C.

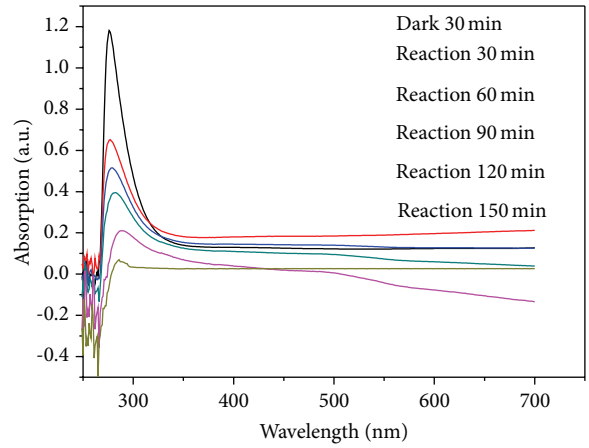

FIGURE 6: Absorption spectra of acephate per 30 min time intervals.

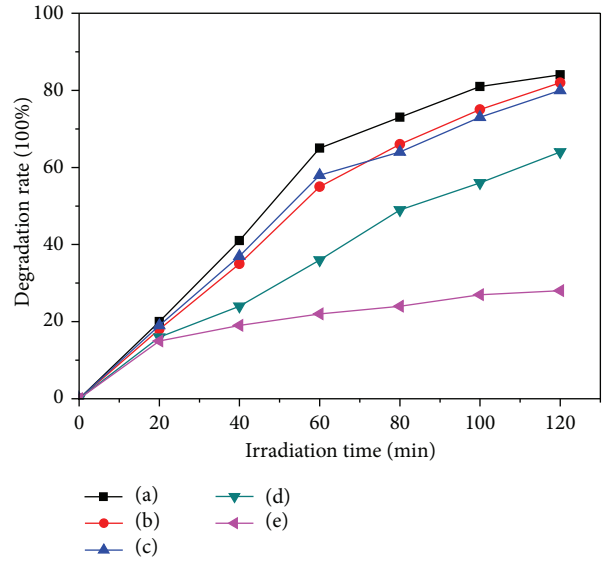

FIGURE 7: Acephate photodegradation rate curves of different samples: N-TiO_2 nanotube arrays annealed at (a) 500°C, (b) 600°C, and (c) 400°C, (d) pure TiO_2 nanotube arrays, and (e) blank.

the Ti is still in the O–Ti–O structure and provides indirect evidence that N exists in the TiO_2 lattice in the form Ti–O–N–O.

3.4. UV-Vis Diffuse Reflectance Spectra Analysis. Figure 5 compares the light absorption properties between pure TiO_2 and N-doped TiO_2 nanotube arrays. The main absorption wavelength of TiO_2 nanotube arrays corresponded to the intrinsic absorption of anatase phase TiO_2, whereas at the optical absorption band edge of N-doped TiO_2 nanotube arrays varying degrees of red shift occurred. The red shift was strongest for the sample annealed in N_2 atmosphere at 500°C. After N doping into TiO_2, the 2p orbital electronic state of the N element overlaps with the O element forming a new valence band. The valence band shifts toward the conduction band and narrows the bandgap. Thus, upon optical excitation, the energy required for the electrons to transit from the valence band to the conduction band decreases leading to a red shift in the absorption edge of N-doped TiO_2 nanotube arrays. This result suggests that, after doping with N, the sunlight utilization of TiO_2 nanotubes is enhanced and the wavelength range of their optical response is expanded. This improves their photocatalytic properties.

3.5. Photocatalytic Activity. Figure 6 shows the UV-vis absorption spectra of acephate solution at different time intervals under the sunlight. At 60 min, the acephate absorbance reached 0.6425 at 270 nm, and the final degradation product showed basically no absorption when the degradation reaction was completed. Xi et al. [18] have reported that the degradation of acephate starts from C–N bond breaking and then it proceeds with gradual oxidation of P–N, P–S, and P–C bonds. Low toxicity intermediates and nontoxic intermediates are produced in the experiment, and as the reaction continues the acephate is eventually mineralized completely. This produces nontoxic small molecules including SO_4^{2-}, NO_3^-, PO_4^{3-}, H_2O, and CO_2 with no secondary pollution.

Figure 7 illustrates the time course of acephate degradation rates under the visible light for different samples under the same conditions. Under the visible-light irradiation, acephate gradually degraded. After adding TiO_2 nanotube arrays photocatalyst, the degradation rate reached more than 60% within two hours. With the N-doped TiO_2 nanotube photocatalyst, the degradation rate was substantially increased to over 80% within two hours. The photocatalytic activity of the samples annealed at 500°C was the strongest and the degradation rate reached 84%.

4. Conclusion

Here N-doped TiO_2 nanotube arrays were prepared by anodic oxidation and then annealed in a N_2 atmosphere. The N doping results in a red shift of the absorption band edge of the TiO_2 nanotube arrays, substantially enhancing the absorption of the visible light. The degradation of acephate

under the visible light shows that the N doping improves photocatalytic efficiency of TiO_2 nanotube arrays. The degradation rate was over 80% within two hours. The photocatalytic activity of samples annealed at 500°C was the strongest with a degradation rate of 84%. Our results provide a theoretical basis for the photocatalytic degradation of acephate under the visible light.

Conflict of Interests

The authors declare that there is no conflict of interests regarding the publication of this paper.

Acknowledgments

The authors thank Henan Province Key Discipline of Applied Chemistry (201218692), Innovation Scientists and Technicians Troop Construction Projects of Henan Province (2013259), Scientific and Technological Department Project of Henan Province (132102210193), and Education Department Project of Henan Province (12A150029).

References

[1] O. Carp, C. L. Huisman, and A. Reller, "Photoinduced reactivity of titanium dioxide," *Progress in Solid State Chemistry*, vol. 32, no. 1-2, pp. 33–177, 2004.

[2] H. L. Li, L. X. Cao, W. Liu, G. Su, and B. Dong, "Synthesis and investigation of TiO_2 nanotube arrays prepared by anodization and their photocatalytic activity," *Ceramics International*, vol. 38, no. 7, pp. 5791–5797, 2012.

[3] R. Asahi, T. Morikawa, T. Ohwaki, K. Aoki, and Y. Taga, "Visible-light photocatalysis in nitrogen-doped titanium oxides," *Science*, vol. 293, no. 5528, pp. 269–271, 2001.

[4] N. Murakami, T. Chiyoya, T. Tsubota, and T. Ohno, "Switching redox site of photocatalytic reaction on titanium(IV) oxide particles modified with transition-metal ion controlled by irradiation wavelength," *Applied Catalysis A: General*, vol. 348, no. 1, pp. 148–152, 2008.

[5] J. Ma, M. Yang, Y. Sun et al., "Fabrication of Ag/TiO_2 nanotube array with enhanced photo-catalytic degradation of aqueous organic pollutant," *Physica E: Low-Dimensional Systems and Nanostructures*, vol. 58, pp. 24–29, 2014.

[6] S. Zhou, T. Matsuoka, Y. Shimotsuma et al., "Localized control of lightmatter interactions by using nanoscale asymmetric TiO_2," *Nanotechnology*, vol. 23, no. 46, Article ID 465704, 2012.

[7] S. S. Kalanure, S. H. Lee, Y. J. Hwang, and O. Joo, "Enhanced photoanode properties of CdS nanoparticle sensitized TiO_2 nanotube arrays by solvothermal synthesis," *Journal of Photochemistry and Photobiology A: Chemistry*, vol. 259, pp. 1–9, 2013.

[8] W. B. Chen, Z. J. Ma, X. L. Pan et al., "Core@dual-shell nanoporous SiO_2-TiO_2 composite fibers with high flexibility and its photocatalytic activity," *Journal of the American Ceramic Society*, vol. 97, no. 6, pp. 1944–1951, 2014.

[9] Y. L. Zhao, D. M. Song, Y. H. Qiang, X. Q. Gu, L. Zhu, and C. B. Song, "Dye-sensitized solar cells based on TiO_2 hollow spheres/TiO_2 nanotube array composite films," *Applied Surface Science*, vol. 309, pp. 85–89, 2014.

[10] T. Ohno, M. Akiyoshi, T. Umebayashi, K. Asai, T. Mitsui, and M. Matsumur, "Preparation of S-doped TiO_2 photocatalysts and their photocatalytic activities under visible light," *Applied Catalysis A: General*, vol. 265, no. 1, pp. 115–121, 2004.

[11] M. Maeda and T. Watanabe, "Visible light photocatalysis of nitrogen-doped titanium oxide films prepared by plasma-enhanced chemical vapor deposition," *Journal of the Electrochemical Society*, vol. 153, no. 3, pp. 186–189, 2006.

[12] T. C. Jagadale, S. P. Takale, R. S. Sonawane et al., "N-doped TiO_2 nanoparticle based visible light photocatalyst by modified peroxide sol-gel method," *Journal of Physical Chemistry C*, vol. 112, no. 37, pp. 14595–14602, 2008.

[13] H. Jia, C. Xu, J. Wang, P. Chen, X. Liu, and J. Qiu, "Synthesis of NaYF4:Yb-Tm thin film with strong NIR photon up-conversion photoluminescence using electro-deposition method," *CrystEngComm*, vol. 16, no. 19, pp. 4023–4028, 2014.

[14] R. P. Vitiello, J. M. Macak, A. Ghicov, H. Tsuchiya, L. F. P. Dick, and P. Schmuki, "N-Doping of anodic TiO_2 nanotubes using heat treatment in ammonia," *Electrochemistry Communications*, vol. 8, no. 4, pp. 544–548, 2006.

[15] K. Shankar, K. C. Tep, G. K. Mor, and C. A. Grimes, "An electrochemical strategy to incorporate nitrogen in nanostructured TiO_2 thin films: modification of bandgap and photoelectrochemical properties," *Journal of Physics D: Applied Physics*, vol. 39, no. 11, pp. 2361–2366, 2006.

[16] B. Mattias, H. M. Erie, and D. Ulrike, "Influence of nitrogen doping on the defect formation and surface properties of TiO_2 rutile and anatase," *Physical Review Letters*, vol. 103, no. 26, pp. 1–4, 2006.

[17] T. Ohno, Z. Miyamoto, and K. Nishijima, "Sensitization of photocatalytic activity of S- or N-doped TiO_2 particles by adsorbing Fe^{3+} cations," *Applied Catalysis A: General*, vol. 302, no. 1, pp. 62–68, 2006.

[18] H. L. Xi, S. T. Han, and Y. J. Zuo, "Photocatalytic degradation of O, S-dimethyl acetyl phosphoramidothioate," *Environmental Chemistry*, vol. 27, no. 5, pp. 559–564, 2008.